Communication

Practical factors in neonatal lung imaging using electrical impedance tomography

A. Taktak P. Record R. Gadd P. Rolfe

Keele University, Department of Biomedical Engineering & Medical Physics, Thornburrow Drive, Hartshill, Stoke-on-Trent ST4 7QB, UK

Keywords—*Electrical impedance tomography, Electrode harnesses, Paediatrics, Respiratory*

Med. & Biol. Eng. & Comput., 1995, **33**, 202–205

1 Introduction

IN NEWBORN infants, hyaline membrane disease, meconium aspiration and pneumonia may cause severe respiratory distress with alterations in lung mechanics. Assessment of the lung function in infants receiving intensive care suggests that measurement of dynamic compliance may provide useful information about the severity of lung disease, prognosis and the likelihood of complications (GREENHOUGH and MORLEY, 1986). At present, there is no technique available to study regional changes in lung volume versus compliance both non-invasively and at the cot side. The development of electrical impedance tomography (EIT) (BARBER *et al.*, 1983) could allow this. EIT also has the potential to monitor lung expansion continuously on a real-time basis. Continuous monitoring will allow the early detection of pneumothorax, airway obstruction and localised lung collapse, conditions which normally lead to deficiency in blood oxygen and ultimately to brain damage.

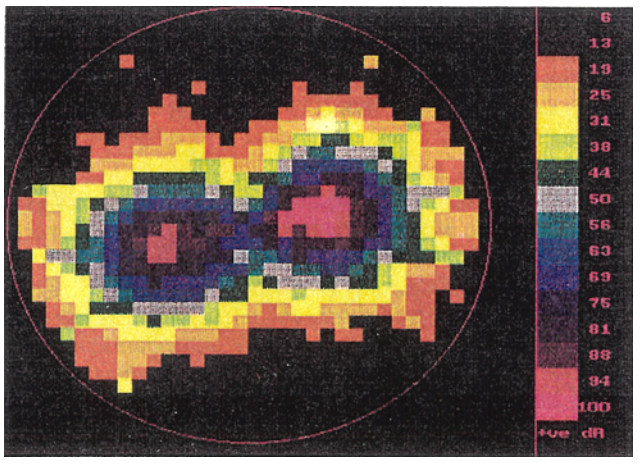

Fig. 1 *Image of healthy adult lungs with 16 levels of intensity: orientation top anterior*

First received 8 February 1994 and in final form 19 April 1994

In this work we try to identify factors that might hinder electrical impedance imaging of the lungs in newborn infants and suggest simple practical solutions.

2 Keele system

The Keele tomograph Mk1b applied 1.5 mA peak-to-peak current at a carrier frequency of 20 KHz, using 16 equidistant electrodes around the object (GADD *et al.*, 1990; RECORD *et al.*, 1990; 1991). Reciprocity errors were measured as described by Rosell *et al.* (ROSELL *et al.*, 1989) but with a slight modification. Rosell used the following equation in determining the reciprocity errors:

$$e = \frac{Z_{12} - Z_{21}}{Z_{12}}$$

where Z_{12} is the impedance calculated from dividing the voltage measured at port 2 while applying the current at port 1, and Z_{21} is the impedance calculated from dividing the voltage measured at port 1 while applying the current at port 2.

Our slight modification was to substitute the denominator by the mean value of Z_{12} and Z_{21} as it was not known which of the two was the correct value.

Reciprocity errors measured on a resistor ring and a resistor phantom were 0.1% and 0.9%, respectively, for an adjacent drive strategy. The common mode rejection ratio (CMRR) of the system was limited by the ON resistance of the CMOS multiplexers, and the CMR figure measured for the front end (up to the electrodes) was better than 60 dB, providing 0.1% measurement accuracy (RECORD *et al.*, 1990). RECORD *et al.* also showed that the use of common mode feedback caused phantom reactances due to overcompensating, and so this was not employed.

Images obtained on an adult chest using the Keele tomograph are shown in Fig. 1. The images were reconstructed using a sensitivity coefficient back-projection algorithm (GADD *et al.*, 1992). Reciprocity errors measured had a mean value of 9%. Certain practical limitations were considered before the technique was applied to the

Fig. 2 *Type (ii) electrode harness*

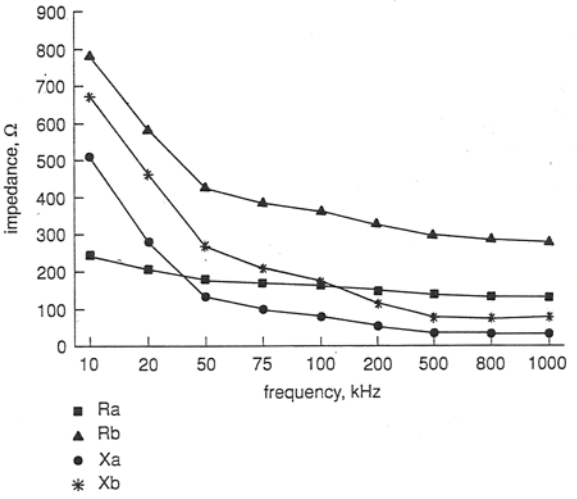

Fig. 3 *Skin contact impedance measurements for RES rubber electrodes and biotrace Ag/AgCl electrodes*

neonates. The first and most obvious problem was the size of the babies. Chest diameters of ten infants were measured and it was found that, on average, they had a circumference of 25.8 ± 4.3 cm. A minimum distance of separation of 10 mm between electrodes was thought necessary to prevent electrolytic bridging. Electrode widths must therefore be ≤ 6 mm, introducing high impedances.

The second problem encountered was the method of applying the electrode. In the adults, electrodes are applied individually. Applying 16 electrodes to the neonates chest, however, requires too much handling of the neonate. A special array was therefore contemplated, to accommodate anatomical differences and not to impede chest expansion in spontaneous breathing.

3 Electrode design

Two types of harnesses were constructed.

3.1 *Type (i)*

This type was assembled with a bandage material used in the maternity ward called Coban*. This material is very stretchy and has the property of only sticking to itself but not to skin. Custom-made 5 mm wide non-sticky non-gelled rubber electrodes were affixed to a Coban strip. The strip was wrapped around the baby's chest twice to firmly hold the electrodes in position. Connection to the front end was achieved by inserting metal pins with a 1 mm diameter inside the electrodes. Screen-driven wires were attached to the end of the pins, thereby providing shielding all the way to the electrodes. The cables had a capacitance of $60\ \text{pF m}^{-1}$ and a mean resistance of $4 \pm 1\ \Omega$. Common mode errors introduced by the harness were therefore not too large.

The first electrode was applied to the anterior side, and the belt was stretched to fit around the baby's chest. Wet gel was applied to the individual electrodes with the aid of a pastic syringe and a disposable pipette tip. Although this was a relatively cumbersome task, the harness had the advantages of simplifying the procedure of positioning the electrodes at the same intercostal level and equidistantly around the baby's chest. The belt also helped achieve firm yet comfortable contact with the baby.

3.2 *Type (ii)*

Electrodes with stud and eyelet connectors were used in this type. Paediatric electrodes Biotrace-NS were recommended by the nursing staff for two reasons. First, they had firm non-irritant adhesion to the skin using Karaya gum, and secondly, they could be cut to relatively small sizes. Unfortunately, the smallest size they could be cut to was 10 mm. This meant that only chest diameters ≥ 32 cm could be measured with this type. The female connectors were recessed in wells made from a padding material called Kushionflex† usually used in the orthopaedic area. When the electrodes were clipped on, their surfaces were flush with the top of the wells, requiring the application of a slight pressure for attachment. This allowed the positioning of the electrodes before applying them to the skin. The wells were joined together by two one-strand elastic bands so as not to apply too much pressure on the baby's chest (Fig. 2).

4 Electrical performance

Large skin-electrode impedances give rise to high potential drops at the skin which might mask voltage changes within the subject (McAdams and Jossinet, 1990; Rosell *et al.*, 1988). Moreover, the presence of reactive impedances generate phase shifts, causing misleading measurements.

Electrode-skin impedance measurement tests described by Riu *et al.* (Riu *et al.*, 1991) were repeated in nine different types of commercial electrodes. As skin impedance depends

Table 1 R_s and C_s values measured for nine types of electrodes at 20 KHz

electrode type	$R_s \pm 10\%$, Ω	$C_s \pm 10\%$, nF
Nico 4535	229	32
Arbo H87V	347	43
Arbo H27V mini	294	41
Biotrace-N	602	29
Biotrace-NS centre snap	580	17
Medicotrace blue sensor	183	42
RES paediatric rubber	204	28
Biotabs2	307	17
EEG	1162	7

* trademark of 3M

† trademark of Smith and Nephew

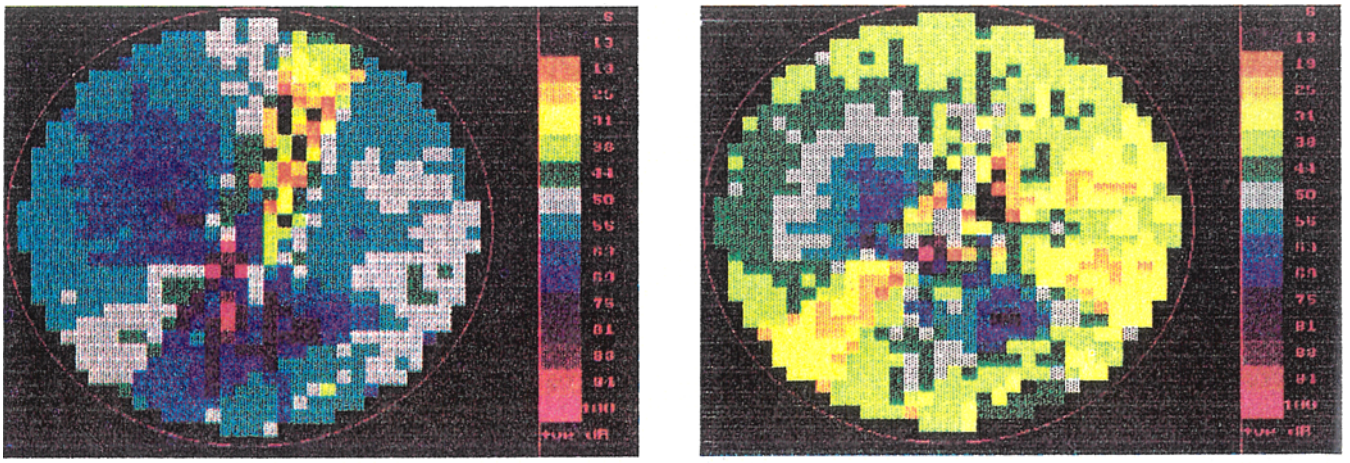

a b

Fig. 4 *Images obtained from premature baby; orientation (a) anterior and (b) posterior*

on a large number of factors such as age, sex, colour, mood, temperature, humidity etc., one subject was examined in the same ambient surroundings in an attempt to stabilise these factors. Tests were carried out on an adult's arm for convenience. The skin impedance varies from one site to another and between subjects (McAdams and Jossinet, 1990; Rosell *et al.*, 1988). Rosell has shown that, in the 10 KHz–1 MHz range, impedance values range from 100 Ω to 5 KΩ. However, comparison of the different electrode interface impedances was still possible as all the tests were carried out on one subject and at the same site. During the tests, movements were restricted to reduce errors caused by the system. Skin impedance was modelled by a resistor R_s, representing the dermal and subcutaneous layers of the skin, in series with a capacitor C_s resembling the dielectric properties of the stratum corneum. The pseudo-capacitance effects of Z_{CPA} (McAdams and Jossinet, 1990) were considered to be insignificant for the range of frequencies studied.

5 Results

The harnesses were assessed by the nursing staff on the maternity ward. Type (i) was preferred in terms of robustness and ease of use. Type (i) was also found to cost less and was easier to construct than type (ii). Impedance measurements showed that the rubber electrodes used in type (i) had better values than the stick-on electrodes used in type (ii) (Fig. 3). At 20 KHz (the carrier frequency for our system), rubber electrodes compared well with other types studied, as shown in Table 1.

The electrode harness type (i) was used to image a 42 days old male baby. The baby had been born prematurely at 30 weeks with a birthweight of 1.68 Kg and had a pneumothorax on the left lung. The baby was ventilated for a period of one month and was presented for testing with EIT four days after he was taken off the ventilator. At this stage, it was not known whether images such as that shown in Fig. 1 could be obtained on babies. The volume of the neonatal chest is approximately 63 times smaller than the adult, and the effective electrical resistance across the baby's chest was anticipated to be higher. In respiratory distress, large physical deformations may occur in the chest of newborn infants. These deformations can cause image distortions in EIT as most reconstruction algorithms have no anatomical corrections.

A block of 32 frames was recorded with a time delay of 32 ms between frames. Measurements had high reciprocity errors (≥40%) due to movement artefacts and unstable contact with the skin. However, obtained images showed some perturbation of high resistivity values. Two frames obtained at different stages during breathing are shown in Fig. 4. The variation in the surrounding colours in Figs. 4*a* and *b* was thought to represent changes in pulmonary blood flow during the respiratory cycle. Orientation deviation of these images from Fig. 1 was probably due to variations in posture and thoracic levels (Harris, 1991).

6 Discussion

Images obtained with electrical impedance tomography have the disadvantage of poor resolution compared to other imaging techniques such as computed tomography (CT) and magnetic resonance imaging (MRI). These techniques provide anatomical images that can be very useful in diagnosis. On the other hand, EIT can provide functional images that allow quantitative and continuous monitoring of the lung mechanics. Other advantages of EIT are the relative low cost and transportability of the equipment which would allow, when fully developed, wide clinical use at the cot side. Safety is another advantage, in that the technique does not involve the use of radiation. These advantages by far outweigh the disadvantage of resolution.

7 Conclusion

Electrical impedance tomography was used in imaging neonatal lungs. Even with high error values caused by movement, chest sizes and attachment difficulties, images with poor resolutions were obtained of a premature baby's lungs at different stages of breathing. Unfortunately, simultaneous respiratory signals were not recorded, and so correlation of these images with breathing was not possible. The effect of posture and thoracic-level factors can only be studied by carrying out a large clinical trial. Narrow rubber electrodes, which were previously considered to have high contact impedances, proved very effective and compared well with different Ag/AgCl types.

Acknowledgment—The authors would like to thank Action Research for funding this project.

References

Barber, D. C., Brown, B. H., and Freeston, I. L. (1983): 'Imaging spatial distributions of resistivity using applied potential tomography,' *Electron. Lett.* **19**, pp. 933–935

Brown, B. H. (1990): 'Overview of clinical applications.' Proc.

Meeting on Electrical Impedance Tomography, European Community Concerted Action on Electrical Impedance Tomography, Copenhagen, Denmark 14–16 July, pp. 29–35
GADD, R., RECORD, P. M., and ROLFE, P. (1990): 'Three dimensional finite element modelling for electrical impedance tomography.' Proc. Meeting on Electrical Impedance Tomography. European Community Concerted Action on Electrical Impedance Tomography, Copenhagen, Denmark, 14–16 July. pp. 71–75
GADD, R., RECORD, P. M., and ROLFE, P. (1992): 'A sensitivity region reconstruction algorithm using adjacent drive current injection strategy,' *Clin. Phys. Physiol. Meas.*, **13**, *A*, pp. 101–105
GREENOUGH, A., and MORLEY, C. J. (1986): 'Is the measurement of compliance useful for clinical management in preterm infants?' *in* ROLFE, P. (Ed.) Neonatal physiological measurements' (Butterworths, London) pp. 261–267
HARRIS, N. D. (1991): 'Applications of electrical impedance tomography in respiratory medicine.' PhD Thesis, Sheffield University, UK
MCADAMS, E. A., and JOSSINET, J. (1990): 'Electrode-skin impedance in impedance tomography.' Proc. Meeting on Electrical Impedance Tomography, European Community Concerted Action on Electrical Impedance Tomography, Copenhagen, Denmark, 14–16 July, pp. 14–19
RECORD, P., GADD, R., and ROLFE, P. (1990): 'A signal conditioning electrode for use in electrical impedance tomography.' Proc. Meeting on Electrical Impedance Tomography, European Community Concerted Action on Electrical Impedance Tomography, Copenhagen, Denmark, 14–16 July, pp. 168–174
RECORD, P. (1991): 'Electrical impedance tomography: methods of improving image quality.' SERC Final Report, Grant GR/E27201
RIU, P. J., LOZANO, A., FERNÀNDEZ, M., and PALLÀS, R. (1991): 'Electrode requirements for electrical impedance tomography.' IV Int. Symp. on Biomedical Engineering, Peńiscola, Spain, pp. 141–142
ROSELL, J., COLOMINAS, J., RIU, P., PALLÀS, R., and WEBSTER, J. G. (1988): 'Skin impedance from 1 Hz to 1 MHz,' *IEEE Trans.*, **BME-35**, pp. 649–651
ROSELL, J., RIU, P., LOZANO, A., and PALLÀS, R. (1989): 'Errors and sensitivity in multielectrode systems for electrical impedance imaging.' Proc. Mediterranean Conf. on Biomedical Engineering, Patras, Greece

Communication

Three-dimensional kinematic angle measurement system for non-jointed rigid axes

P. T. Kolen

Electrical and Computer Engineering Department, Electromagnetic Instrumentation Design Laboratory, San Diego State University, San Diego CA 92182-0190, USA

Keywords—*Angle measurement, Goniometer, Hall generators.*

Med. & Biol. Eng. & Comput., 1995, **33**, 205–211

1 Introduction

MOST, IF not all, biomechanical angular measurements are made using some form of goniometer. The most common form of goniometer utilises a coaxial rotary sensor, i.e. potentiometers or optical encoders. This class of goniometer is limited to one-dimensional angular measurements of two rigid axes joined at a common hinge joint. A commercially available unit extends the fixed joint approach to two-dimensional angular measurements, i.e. ball joints, by employing a two-axis linear strain gauge. Although useful for this type of angular measurement, fixed axis goniometers are subject to errors introduced by misalignment of the sensor and joint rotation axis. To overcome the problem of joint/sensor alignment, multiple accelerometer configurations have been used with some success (MITEL and KING, 1979; MORRIS, 1973; SMIDT *et al.*, 1977; WILLEMSEN *et al.*, 1990).

Unlike the coupled axis situation described above, rigid axes that do not share a common joint cannot utilise the conventional goniometer approach. Alternatively, each axis must be independently referenced to a common frame of reference from which the relative orientations can be deduced. Previous attempts at creating an external frame of reference utilised a fixed localised artificial magnetic field. A sensing coil affixed to the moving axis provided a usable signal to allow the calculation of the relative orientation between the field and coil (RAAB *et al.*, 1979). In practice, this approach proved to be impractical due to the complex iterative calculations required to remove the spatial variations inherent in the artificial magnetic field. Additionally, the rapid fall-off of field strength limited the range of motion to a small spatial volume.

It has been successfully demonstrated that a Hall effect-based sensor system referenced to the earth's ambient magnetic field can be used to measure the three-dimensional angular relation between arbitrary rigid axes (KOLEN *et al.*, 1993). By calculating the three-dimensional angular orientation of the individual axes referenced to the fixed external magnetic field vector, the relative angular relationship between any number of independent axes can be easily calculated. The calculational effort needed to derive the relative angular information is relatively simple due to the high degree of spatial uniformity of the ambient magnetic field over a large volume of space. This field consistency eliminates the computation-intensive algorithms required to remove the effects of field geometry variations inherent in the afore-mentioned locally generated magnetic transmitter/receiver-based system.

The primary difficulty in implementing a Hall effect sensor

First received 10 July 1992 and in final form 6 April 1994